Journal of Applied Polymer Science

Synthesis of poly(ester amide)s composed of lactic acid and glycolic acid units by the bulk polycondensation of metal halide salts

Sara K. Murase, Jordi Puiggalí
Departament d'Enginyeria Química, Universitat Politècnica de Catalunya, Avenida Diagonal 647, Barcelona E-08028, Spain
Correspondence to: J. Puiggalí (E-mail: jordi.puiggali@upc.es)

ABSTRACT: Thermal polycondensation of the potassium salt of *N*-methylchloroacetyl-6-aminohexanoic acid (LAHK) was found to be effective in the preparation of a new poly(ester amide) based on lactic acid units with a high yield and a moderate molecular weight. The reaction started in the solid state and proceeded through the formation of potassium chloride salt as the driving force. The use of a monomer having an amide linkage diminished the secondary reactions previously found in the synthesis of polylactide from 2-halogenopropionates. The polymerization of potassium salt of *N*-chloroacetyl-6-aminohexanoic acid (GAHK) took place in a similar temperature range as that of the 2-chloropropionyl derivative; in this way, it was possible to conduct the copolymerization processes. The polymerization kinetics of LAHK and its mixture with GAHK was studied by Fourier transform infrared spectroscopy. The bulk polycondensation reaction was faster for GAHK than for LAHK, but the kinetic differences were not significant enough to prevent copolymerization at a temperature close to 160°C. Therefore, new degradable materials with tuned properties according to the glycolic acid/lactic acid content were obtained. ^{1}H-NMR spectroscopy was useful for following the time evolution of the copolymerization process and for determining the final composition. Calorimetric data showed that all of the samples were thermally stable and that decreases in the melting temperature and enthalpy were observed at intermediate compositions. The existence of an eutectic point became proof that effective copolymerization was achieved in the thermal polycondensation process. © 2015 Wiley Periodicals, Inc. J. Appl. Polym. Sci. **2016**, *133*, 43197.

KEYWORDS: biodegradable; copolymers; synthesis and processing

Received 7 July 2015; accepted 9 November 2015
DOI: 10.1002/app.43197

INTRODUCTION

It is well known that the solid-state reaction of halogenoacetates ($XCH_2COO^-M^+$) leads to the formation of polyglycolide by the elimination of the metal halide salt (X^-M^+); this can be considered as a driving force for the polycondensation process, which is a highly favorable thermodynamic process.[1–3] In fact, the polymerization reaction is highly exothermic as a consequence of the large lattice energy of the formed metal halide, which has a reactivity that is higher with the use of large metal cations (e.g., Cs^+) and small halogen anions (e.g., Cl^-). Despite the great simplicity of this method, it has a strong limitation caused by thermal degradation, which leads to a maximum degree of polymerization that is close to 40 (i.e., a number-average molecular weight near 2000 g/mol).

The previously described solid-state reaction has also been applied to prepare aliphatic polyesters, such as polylactide,[4] poly(3-hydroxypropionate),[4] and poly(2-hydroxybutyric acid),[5] from 2-halogeno-propionates, 3-halogenopropionates, or 2-halogenobutyrates, respectively. In general, worse results were attained in these cases because of different types of secondary reactions. Thus, for example, the polymerization of sodium 3-chloropropionate was affected by the competitive intramolecular elimination of NaCl, which led to the formation of acrylic acid. In the same way, the polymerization of sodium 2-chloropropionate gave rise to a great proportion of volatile lactide through the pyrolysis of previously formed polylactide.

Studies performed on the polymerization of 2-chloropropionates also revealed that the selected metal cation was fundamental in allowing the polycondensation process. Thus, the polymerization was thermodynamically favorable for sodium compounds but not for lithium derivatives; this was also corroborated experimentally.[6] Copolyesters containing glycolic acid and lactic acid units were also prepared by the thermal reaction of crystal mixtures of sodium or potassium chloroacetates and sodium or potassium 2-chloropropionates. The products were always lactic acid terminated block copolymers, again with low molecular weights.[6] Although this kind of reaction starts in the solid state, liquefaction usually occurs, as in the case of copolymers incorporating more than 10 mol % lactide. Basically, a true solid-state

polymerization is only possible when the reaction temperature becomes lower than the melting point of the formed polymer, a feature that is feasible for polyglycolide, whose melting temperature is close to 215°C.

Later studies demonstrated that adverse secondary reactions could be minimized with a halogenocarboxylate salt with an internal amide group as a monomer. The method allows the preparation of biodegradable poly(ester amide)s (PEAs) with good yield and a moderate molecular weight. Thus, solid-state polymerization was successfully performed with metal salts of *N*-chloroacetyl-ω-amino acids,[7,8] and the process was even extended to attain PEAs from mixtures of a *N,N′*-bis(chloroacetyl) diamine and a dicarboxylate metal salt.[8] It should be pointed out that PEAs currently constitute an interesting alternative to polyesters,[9–12] which are considered the most important family of biodegradable materials so far for both commodity and specialty applications. In fact, PEAs can combine a degradable character, afforded by their hydrolyzable ester groups, with the relatively good thermal and mechanical properties given by the strong intermolecular hydrogen-bonding interactions that can be established between their amide groups.

The thermal polycondensation procedure has been studied extensively to prepare PEAs constituted by glycolic acid units; this proves the capability of obtaining functionalized PEAs with protected L-lysine as a diamine,[13] branched PEAs as biodegradable coatings,[14] and PEAs having a variable glycolic acid comonomer content to achieve a tuned degradability.[15] Furthermore, the presence of an inorganic salt byproduct is also interesting, as previously reported[1–3] because it can be removed by extensive washing with water; this gives rise to a highly porous material that could be relevant for some biomedical applications. Specific studies have also been performed to demonstrate also the hydrolytic and enzymatic degradability of PEAs constituted by glycolic acid units and ω-amino acids[16] and by glycolic acid units, amines, and dicarboxylic acid units.[17]

Despite the intense research performed with PEAs derived from glycolic acid, studies referring to thermal polycondensation to produce lactic acid derivatives are scarce.[18,19] This study was focused on the suitability of synthesizing PEAs incorporating acid lactic units by means of a method based on metal halide formation. In this way, the evaluation of the polymerization kinetics of the potassium salt of *N*−2-chloropropionyl-6-aminohexanoic acid (LAHK: L for lactic unit, AH for aminohexanoic, and K for potassium) and characterization of the corresponding PEAs were carried out. Furthermore, copolymerization with the potassium salt of *N*-chloroacetyl-6-aminohexanoic acid (GAHK: G for glycolic unit, AH for aminohexanoic, and K for potassium) was also considered because a series of copolymers having different glycolic acid/lactic acid ratios and tunable properties could be easily obtained, whereas the same amino acid (i.e., 6-aminohexanoic) was used. Both the stereoregularity and chain regularity were lost as a consequence of copolymerization. Synthesis schemes for the LAHK monomer and the corresponding P(GAH–LAH) *x* copolymers (where P denotes the polymer and *x* denotes the theoretical molar ratio of GAH) are shown in Figure 1.

EXPERIMENTAL

Materials

Chloroacetyl chloride, 2-chloropropionyl chloride (97%), 6-aminohexanoic acid (≥98.5%), sodium hydroxide (NaOH; pellets), potassium hydroxide (KOH; pellets, ≥85%), ethyl acetate, and formic acid (≥95%) were purchased from Sigma-Aldrich and were used as received. Toluene (≥99.8%), diethyl ether (≥99.8%), and ethanol (EtOH) were purchased from Panreac. *N*-Chloroacetyl-6-aminohexanoic acid was obtained as previously reported.[8] The corresponding potassium salt was prepared by neutralization with a 4*M* KOH ethanolic solution.

Synthesis of the LAHK Monomer

***N*-Methylchloroacetyl-6-aminohexanoic Acid (LAH Acid).** In the first step [Figure 1(a)], 0.11 mol (10.68 mL) of 2-chloropropionyl chloride was dissolved in 15 mL of diethyl ether under a nitrogen atmosphere in a previously dried pressure-equalizing dropping funnel. The solution was added dropwise to 30 mL of a 4*M* solution of NaOH containing 13.1 g (0.1 mol) of 6-aminohexanoic acid in a round-bottomed flask with magnetic stirring at a temperature of 0°C. The pH of the solution was kept around 11 by the dropwise addition of 4*M* NaOH to favor the elimination of the formed HCl. The solution was then acidified until it reached pH 1.5 with a 2*M* HCl solution; the temperature was kept at 0°C. The final solution was extracted with ethyl acetate and rotavaporated to recover a white product (LAH acid), which was recrystallized in toluene.

Yield = 65%. Fourier transform infrared (FTIR) spectroscopy–attenuated total reflection (ATR; cm^{-1}): 3275 (amide A); 3105 (amide B); 2972, 2944, and 2865 (CH_2); 1652 (amide I) and 1572 (amide II). ^{1}H-NMR [$CDCl_3$, tetramethylsilane (TMS) as internal reference, ppm]: 6.62 (s, 1H, CON*H*CH_2), 4.45–4.38 [m, 1H, C*H*(CH_3)CO], 3.33–3.26 (m, 2H, CONHC*H*$_2$), 2.37 (t, J = 7.3 Hz, 2H, C*H*$_2$COOH), 1.74 [d, J = 7.1 Hz, 3H, ClCH(C*H*$_3$)], 1.70–1.62 (m, 2H, CONHCH$_2$C*H*$_2$), 1.60–1.52 (m, 2H, C*H*$_2$CH$_2$COOH), 1.44–1.34 (m, 2H, CH$_2$CH$_2$C*H*$_2$CH$_2$CH$_2$).

LAHK. The obtained LAH acid crystals were dissolved in EtOH at 0°C, and a 4*M* KOH ethanolic solution was added dropwise until basic pH was reached. The potassium salt precipitated immediately as a white solid, which was washed extensively with EtOH and dried *in vacuo*.

Yield = 92%, mp = 177°C. FTIR–ATR (cm^{-1}): 3290 (amide A), 3091 (amide B), 2929 and 2860 (CH_2), 1658 (amide I), 1556 (amide II). ^{1}H-NMR [dimethyl sulfoxide (DMSO), TMS as the internal reference, ppm]: 6.62 (t, J = 6.9 Hz, 1H, CON*H*CH_2), 4.59–4.52 [m, 1H, C*H*(CH_3)CO], 3.07–3.00 (m, 2H, CONHC*H*$_2$), 1.81 (t, J = 7.2 Hz, 2H, C*H*$_2$COO$^-$K$^+$), 1.50 [d, J = 5.7 Hz, 3H, ClCH(C*H*$_3$)], 1.45–1.33 (m, 4H, CH$_2$C*H*$_2$CH$_2$C*H*$_2$CH$_2$), 1.30–1.16 (m, 2H, CH$_2$CH$_2$C*H*$_2$CH$_2$CH$_2$).

Polymerization Process [P(GAH–LAH) *x*]

Copolymerizations were carried out on a preparative scale by the heating of an appropriate mixture of mortared potassium salts to 160°C in a previously dried and N_2-purged reaction tube provided with a magnetic stirrer. The reaction time was 90 min because the complete reaction of the less reactive LAHK

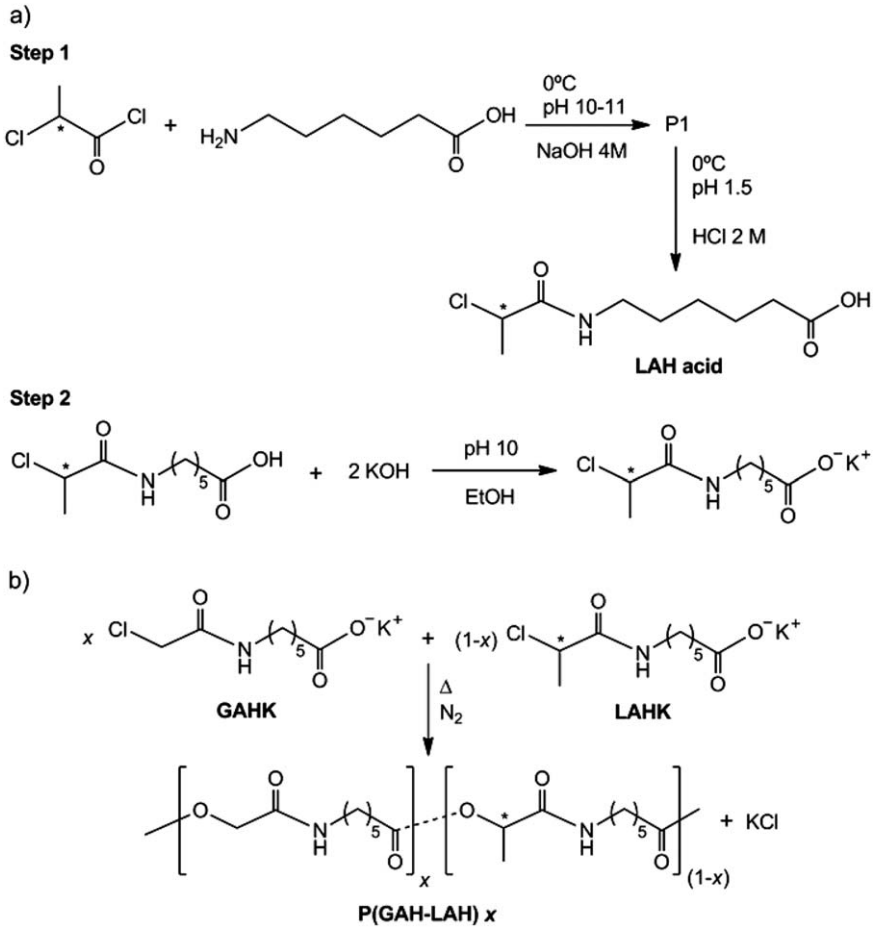

Figure 1. Synthesis schemes for the (a) LAHK lactic acid based monomer and (b) P(GAH–LAH) *x* copolymers prepared with an *x* molar fraction of the GAHK glycolic acid monomer. "Note that homopolymers derived from glycolic acid and lactic acid can also be named as PGAH and PLAH, respectively".

monomer was assured and no degradation evidence was detected with this time.

In all cases, the polycondensation reaction finished and mainly proceeded in the liquefied state. After cooling, the lactide homopolymer [i.e., P(GAH–LAH) 0] and copolymers were separated from potassium chloride by precipitation from a formic acid solution with EtOH. The recovered solid was extensively washed with water, EtOH, and ethyl ether to obtain a white powder (yield = 62–74%), which was stored *in vacuo*. Spectroscopic data were always consistent with the expected chemical structure of the polymer, as indicated for the P(GAH–LAH) 0 sample:

FTIR–ATR (cm^{-1}): 3289 (amide A), 3095 (amide B), 2937 and 2865 (CH_2), 1740 (C═O), 1654 (amide I), 1548 (amide II), 1157 (C—O). ^{1}H-NMR (DMSO, TMS as the internal reference, ppm): 8.02 (s, 1H, CON*H*CH_2), 4.91–4.84 [m, 1H, OC*H*(CH_3)CO], 3.04 (m, 2H, CONHC*H*$_2$), 2.39–2.27 (m, 2H, C*H*$_2$CO), 1.55–1.43 (m, 2H, C*H*$_2$CH$_2$CO), 1.38 (m, 2H, CONHCH$_2$C*H*$_2$), 1.30–1.27 [d, J = 6.8 Hz, 3H, OCH(C*H*$_3$)], 1.24 (m, 2H, CH$_2$CH$_2$C*H*$_2$CH$_2$CH$_2$). ^{13}C-NMR ($CDCl_3$, TMS as the internal reference, ppm): 172.16 (*C*OO), 169.79 (*C*ONH), 69.54 [O*C*H(CH_3)], 38.09 (CONH*C*H$_2$), 33.28 (*C*H$_2$CO), 28.63 (CONHCH$_2$*C*H$_2$), 25.62 [OCH(*C*H$_3$)], 23.96 (*C*H$_2$CH$_2$CO), 17.70 (CH$_2$CH$_2$*C*H$_2$CH$_2$CH$_2$).

Measurements

The molecular weight and polydispersity index were estimated by gel permeation chromatography (GPC) with a liquid chromatograph (Shimadzu, model LC-8A) equipped with the Empower computer program (Waters) and a refractive-index detector (Shimadzu RID-10A). A PL HFIP gel guard precolumn (Polymer Lab) and PL HFIP gel column (Agilent Technologies Deutschland GmbH) were used. The polymer was dissolved and eluted in 1,1,1,3,3,3-hexafluoroisopropanol containing CF_3COONa (0.05*M*) at a flow rate of 0.5 mL/min (injected volume = 100 μL, sample concentration = 1.5 mg/mL). The number- and weight-average molecular weights and molar-mass dispersities were calculated with poly(methyl methacrylate) standards, with a technical error of measurement of less than 10%.

IR absorption spectra were recorded with an FTIR 4100 Jasco spectrometer in the 4000–600 cm^{-1} range. A Specac model MKII Golden Gate ATR instrument set up with a heated

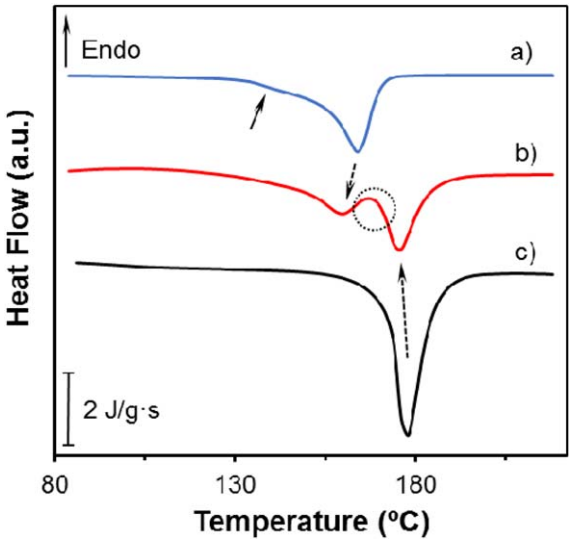

Figure 2. DSC heating traces (20°C/min) for the (a) GAHK and (c) LAHK monomer salts and (b) M(GAHK–LAHK) 50 equimolar monomer mixture. The continuous arrow shows the exothermic shoulder observed for the polymerization of GAHK, whereas the dashed arrows indicate the evolution of exothermic peaks for the copolymerization reaction. The dashed circle indicates peak overlap for the copolymerization process. [Color figure can be viewed in the online issue, which is available at wileyonlinelibrary.com.]

Diamond ATR top plate, which could be used up to 200°C, and a Series 4000 high-stability temperature controller were also used.

A Bruker AMX-300 spectrometer operating at 300.1 and 75.5 MHz was used for ^{1}H-NMR and ^{13}C-NMR investigations, respectively. Chemical shifts were calibrated with TMS as the internal standard. The assignment of methylene protons of the copolymers was corroborated by Heteronuclear correlation spectroscopy (HETCOR) two-dimensional spectra with standard pulse sequences provided by Bruker.

Calorimetric data were obtained by differential scanning calorimetry (DSC) with a TA Instruments Q100 series instrument equipped with a refrigerated cooling system, which operated from −90°C to 550°C. Experiments were conducted under a flow of dry nitrogen with a sample weight of approximately 10 mg, whereas calibration was performed with indium. The heating and cooling runs were carried out at a rate of 20°C/min.

Thermal degradation was studied at a heating rate of 10°C/min with samples of around 10 mg in a Q50 thermogravimetric analyzer (TA Instruments) under a flow of dry nitrogen. The analysis was performed in the 30–600°C temperature range.

RESULTS AND DISCUSSION

Calorimetric Data on the Thermal Polycondensation Process of Metal Halide Salts

DSC heating scans of the GAHK and LAHK monomers showed exothermic peaks indicative of the condensation reaction and the formation of the corresponding metal halide salt (Figure 2). In both cases, the reaction started in the solid state, given that no previous endothermic peak associated with the melting of the monomer crystals was detected.

The DSC trace of GAHK was complex because a small shoulder was observed at a temperature close to 140°C (see continuous arrow) in addition to a clear exothermic peak at 164°C. Solid-state polymerization strongly depends on the crystalline structure of the monomer and specifically on the close arrangement between chloride and potassium ions. It is clear that the temperature at which polymerization starts should depend on the degree of crystalline order and also on the specific structure. Therefore, the existence of different exothermic events should be linked to both different crystal perfections and crystalline structures because the polycondensation process is highly dependent on the way that the monomers are prepared. In this way, the exotherm found at 164°C was in full agreement with the previously reported reaction temperature (i.e., 172°C) for the polycondensation of the GAHK monomer prepared from an EtOH solution.[20] On the contrary, the monomer obtained from aqueous media showed exothermic peaks (i.e., 121 and 130°C) at clearly lower temperatures.[15]

The polymerization of LAHK took place in a narrower temperature range; in this case, we only observed a clear exothermic peak at 177°C. The enthalpy associated with this peak was slightly higher than that determined for the polymerization of GAHK (i.e., 48.5 kJ/mol with respect to 39.7 kJ/mol); this suggested a lower lattice enthalpy for LAHK because, in both polycondensation processes, the same metal halide salt was formed. In any case, the calorimetric data obtained from both monomers suggested the possibility of undertaking a copolymerization process because the corresponding reaction temperatures were close enough (i.e., 164 and 177°C). Thus, the heating trace for the representative equimolar mixture [abbreviated as M(GAHK–LAHK) 50, where M denotes a mixture of monomers and 50 denotes the molar ratio of GAHK] allowed us to verify an exothermic process that covered a wide temperature range (Figure 2) and specifically to detect the events associated with the polymerization of each monomer (i.e., shoulder and peak for GAHK and peak for LAHK). Nevertheless, it was important that we observed that the exothermic peaks overlapped slightly (see dashed circle), a feature that may have justified the existence of glycolic and lactic acid units in the final polymer chain,

Table I. Calorimetric Polymerization Data for Single Monomers and Their Mixtures

Sample	T (°C)	ΔH (J/g)
LAHK	177	173[a]
M(GAHK-LAHK) 20	164	143
M(GAHK-LAHK) 50	160-175	168
M(GAHK-LAHK) 80	127-140	106
GAHK	164	152[b]

Nomenclature: LAHK: L for lactic unit, AH for aminohexanoic, K for potassium; GAHK: G for glycolic unit, AH for aminohexanoic, K for potassium; M denoting mixture of monomers.
[a] 48.5 kJ/mol.
[b] 39.7 kJ/mol.

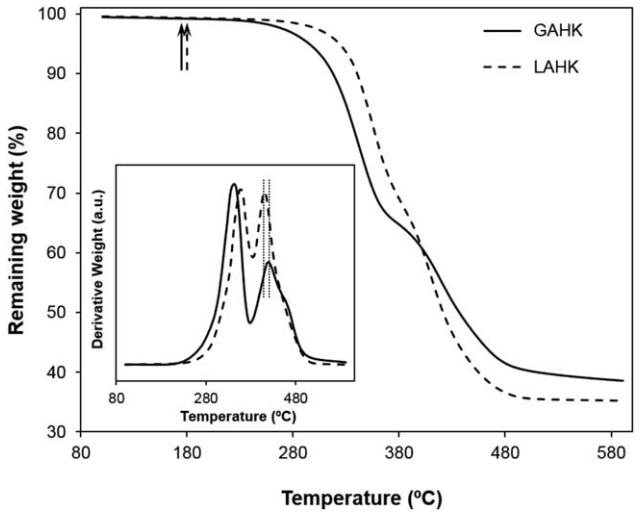

Figure 3. TGA curves for the GAHK and LAHK monomer salts. DTGA curves are displayed in the inset. Continuous and dashed arrows indicate the DSC exothermic peak temperatures determined for GAHK and LAHK, respectively.

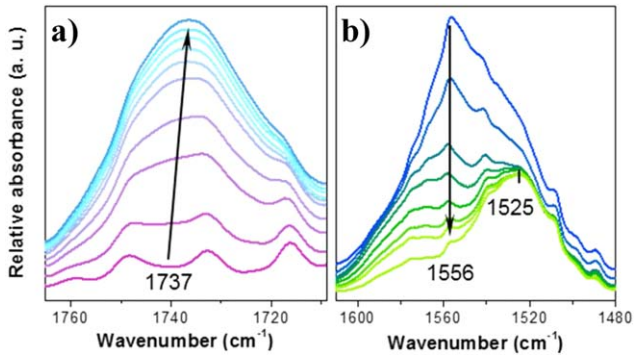

Figure 4. FTIR spectra showing the evolution of representative absorption bands during the polymerization of LAHK at 170°C: appearance and disappearance of (a) carboxylic ester and (b) carboxylate bands, respectively. [Color figure can be viewed in the online issue, which is available at wileyonlinelibrary.com.]

although a block microstructure should have mainly been developed because of the lower reaction temperature of GAHK.

The heating trace of the monomer mixture also showed a slight shift toward lower temperatures of the two exothermic peaks associated with each monomer, a feature that may also have been an indication that a reaction between the monomers took place. Logically, the exothermic enthalpy determined for the polycondensation of the monomer mixture was intermediate of those found for the corresponding monomers. Table I summarizes the DSC calorimetric data obtained from the monomers and the studied mixtures. Basically, mixtures having a predominant monomer [i.e., M(GAHK–LAHK) 20 and M(GAHK–LAHK) 80] exhibited similar behavior to that observed for the principle monomer, with the consideration that both the reaction temperature and the enthalpy decreased.

The thermal stability of both GAHK and LAHK monomers was verified because of the relatively high temperature that was required to conduct the polycondensation reaction (164–177°C). The thermogravimetric analysis (TGA) and Differential thermogravimetric analysis (DTGA) curves (Figure 3 and Table II) clearly demonstrated that thermal decomposition started at more than 80°C above the reaction temperature. It should be also taken into account that the DSC data were determined at a high heating rate, and consequently, the isothermal polycondensation processes could be performed at a lower temperature than that corresponding to the exothermic peaks.

The new LAHK monomer was even more stable than the previously studied GAHK salt, as deduced from the onset temperatures reported in Table II (i.e., 279°C with respect to 250°C). Both monomers decomposed after two decomposition steps, with the first one mainly associated with glycolic and lactic acid residues.[18] Greater stability was found for the lactic moiety with respect to the glycolic one, whereas decomposition associated with the 6-aminohexanoic unit appeared to be slightly favored by the former degradation of the lactic acid unit, as was easily deduced from the DTGA curves (Figure 3).

Table II also reports the remaining weight at 550°C, which mainly corresponded to the KCl reaction byproduct. In both cases, the experimental weights were slightly higher than those corresponding to the theoretical amount of salt (i.e., 30 and 29% for the GAHK and LAHK samples, respectively). Thus, organic char was also formed under such experimental conditions; the amount was slightly higher for the glycolic acid derivatives (i.e., 8.6 vs 6.2%).

Polymerization Kinetic Studies through FTIR Data

FTIR spectroscopy has proven to be an ideal technique for obtaining data from the polymerization process of monomer salts because it prevents the possible interference of different events, such as polymer crystallization, that can be detected by means of other techniques, such as typical calorimetric analysis.

We followed the polymerization processes by considering bands belonging to specific groups that were originated by the condensation reaction; these included the C═O absorption band around 1737 cm^{-1}, which was associated with the newly formed ester group [Figure 4(a)]. The absorbance decrease in the band associated with the carboxylate group [1556 cm^{-1}; Figure 4(b)] could also be

Table II. Characteristic TGA Temperatures, Remaining Weights, and DTGA Peak Values for the Decomposition of GAHK and LAHK Monomer Salts

Sample	T_{onset} (°C)	$T_{10\%}$ (°C)	$T_{20\%}$ (°C)	$T_{50\%}$ (°C)	w_t (%)	T_1 (°C)	T_2 (°C)
LAHK	279	340	357	421	35.2	355	410
GAHK	250	317	338	436	38.6	343	418–457

T_1 and T_2, the two temperatures observed in the DTGA traces.

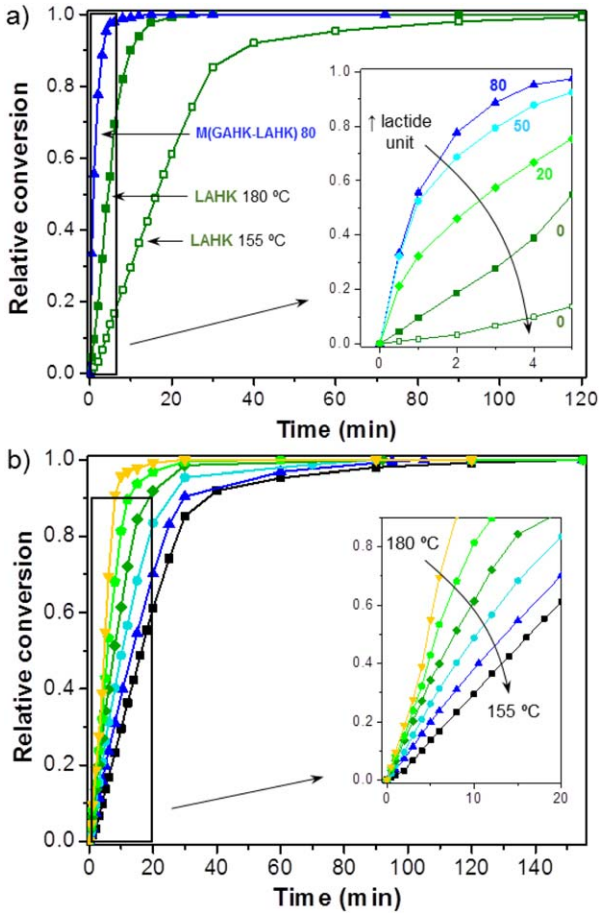

Figure 5. (a) Plots of the relative conversion deduced from the FTIR data during the isothermal polymerization of LAHK at (■) 180 and (□) 155°C. For the sake of completeness, data for the polymerization of the M(GAHK–LAHK) 80 mixture at 175°C are also plotted (▲). The inset shows the evolution of mixtures with 50% GAHK (light blue circles) and 20% GAHK (green rhombus) at the beginning of polymerization. (b) Plots of the relative conversion for the polymerization of LAHK at the indicated isothermal temperatures. [Color figure can be viewed in the online issue, which is available at wileyonlinelibrary.com.]

useful, but its overlap with the invariable amide II band at 1548–1525 cm^{-1} made its use unfeasible for kinetic evaluation purposes.

The relative conversion degree (α_t) for a given reaction time (t) was calculated from absorbance measurements of the band at 1737 cm^{-1} according to eq. (1):

$$\alpha_t = (A_t - A_0)/(A_\infty - A_0) \quad (1)$$

where A_t is the absorbance at time t and A_∞ and A_0 are the final and initial absorbances, respectively.

Figure 5(a) compares the evolution of relative conversion with the reaction time for different monomer mixtures and temperatures. It was clear that the reaction proceeded faster as the GAHK content increased, and the reaction temperature also increased [see also Figure 5(b)]. Thus, 40 min was enough time for the reaction to reach a complete conversion for the less reactive monomer LAHK at a temperature of 180°C, whereas 2 h were required for the polycondensation process to be completed at 155°C.

The reciprocal polymerization half-time ($1/\tau_{1/2}$), calculated as the inverse of the time required to obtain a relative conversion of 0.5, was considered for a preliminary study of the polymerization process. Obviously, an accurate analysis requires the determination of the best kinetic model; this is a specific task that was not undertaken in this study. Also, the kinetic model may change during a polymerization process that starts and finishes in different physical states (i.e., solid at the beginning, where the closeness of reactive groups is fundamental, and liquid at the end, where the mobility of molecules becomes essential). Furthermore, the polymerization half-time ($\tau_{1/2}$) should reflect better the solid-state polycondensation that occurs at low conversion degrees (i.e., <50%).

The evolution of the reciprocal parameter with the polymerization temperature for the new LAHK monomer and the different mixtures is shown in Figure 6, whereas the specific kinetic data are summarized in Table III. These data clearly point out that for a given temperature, the reaction rate increased with the GAHK content in the mixture, with the differences becoming more significant as the reaction temperature increased. Therefore, copolymerization should be performed at low temperatures to prevent a blocky microstructure derived from the faster polycondensation of the GAHK salt. Specifically, a temperature of 160°C was selected for the subsequent polymerizations carried out at a preparative scale because differences in the reaction rate of monomer salts were still acceptable and the time required to achieve complete conversion was not high enough for significant degradation to occur. For example, the complete conversion of LAHK required more than 2 h when the reaction was performed at 155°C [Figure 5(a)]; in this case, we detected some evidence of degradation in the subsequent GPC measurements.

The activation energy for the polymerization process of the LAHK monomer and its mixtures with GAHK salt was calculated with the assumption of a linear dependence between the kinetic constant (k) and the $1/\tau_{1/2}$ parameter and also a typical

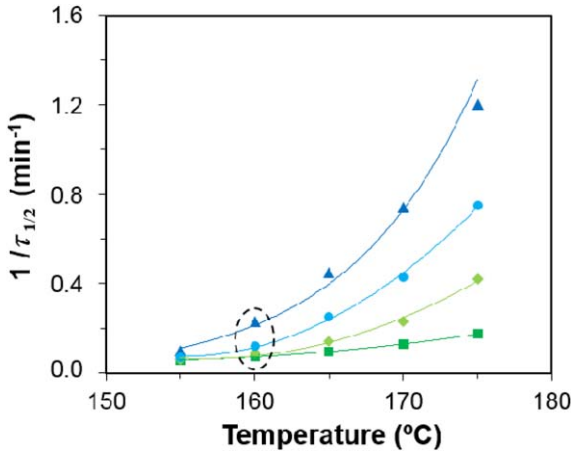

Figure 6. Temperature dependence of $1/\tau_{1/2}$ for (■) LAHK, (◆) M(GAHK–LAHK) 20, (●) M(GAHK–LAHK) 50, and (▲) M(GAHK–LAHK) 80. The dashed ellipse indicates the slight differences determined at 160°C. [Color figure can be viewed in the online issue, which is available at wileyonlinelibrary.com.]

Table III. Kinetic Polymerization Data for LAHK and M(GAHK–LAHK) Monomer Mixtures

Sample	T (°C)	$\tau_{1/2}$ (min)	$1/\tau_{1/2}$ (min^{-1})	E_a (kJ/mol)	$c \times A$ (min^{-1})
LAHK	155	16.9	0.059	86	1.9×10^9
	160	13.7	0.073		
	165	10.3	0.097		
	170	7.8	0.128		
	175	5.7	0.175		
M(GAHK-LAHK) 20	155	16.7	0.060	153	3.3×10^{17}
	160	11.1	0.090		
	165	7.1	0.140		
	170	4.3	0.232		
	175	2.4	0.417		
M(GAHK-LAHK) 50	155	14.3	0.070	192	1.8×10^{22}
	160	8.3	0.120		
	165	4.0	0.250		
	170	2.3	0.435		
	175	1.3	0.769		
M(GAHK-LAHK) 80	155	10.0	0.10	196	9.4×10^{22}
	160	4.3	0.23		
	165	2.2	0.45		
	170	1.4	0.71		
	175	0.8	1.25		

Arrhenius-type relationship between reaction temperature and kinetic constant values:

$$1/\tau_{1/2} = ck = cA \exp - (E/RT) \quad (2)$$

where E, A, c, T and R are the activation energy, the preexponential frequency factor, a constant relating k and $1/\tau_{1/2}$, temperature and the universal gas constant, respectively.

Plots of ln k versus $1/T$ (Figure 7) allowed us to determine the activation energies for the polymerization of LAHK and its mixtures with GAHK (Table III). In all cases, a linear dependence with a high correlation coefficient ($r = 0.988$–0.998) was obtained. The lowest activation energy (86 kJ/mol) was found for LAHK, as also reflected by the lower increase in $1/\tau_{1/2}$ with temperature (Figure 6). The activation energies were practically similar for GAHK contents higher than 50% [e.g., 196 and 192 kJ/mol for M(GAHK–LAHK) 80 and M(GAHK–LAHK) 50, respectively]. It was also interesting to note the great difference between the $c \times A$ values, which reached the highest values for GAHK-rich samples [i.e., 9.4×10^{22} for M(GAHK–LAHK) 80]. The large difference with the value determined for LAHK (i.e., 1.9×10^9) explained the higher polycondensation rate of GAHK and suggested a higher frequency factor; this may have been due to a crystalline structure with a closer disposition of chlorine atoms and potassium ions.

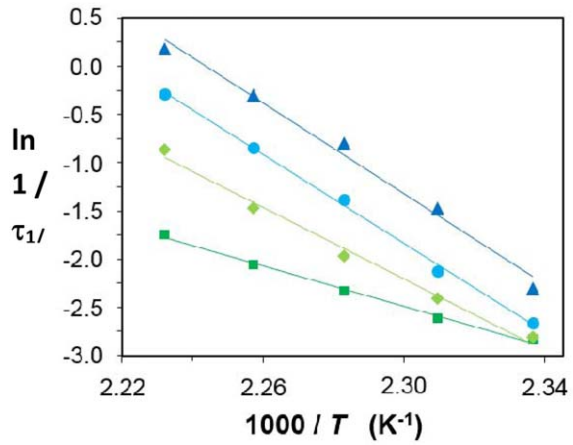

Figure 7. Plots of ln $1/\tau_{1/2}$ versus the reciprocal of the polymerization temperature for (■) LAHK, (◆) M(GAHK–LAHK) 20, (●) M(GAHK–LAHK) 50, and (▲) M(GAHK–LAHK) 80. [Color figure can be viewed in the online issue, which is available at wileyonlinelibrary.com.]

Copolymerization of LAHK and GAHK

To determine the optimal reaction time, GPC chromatograms were obtained during the polycondensation reactions carried out at the previously selected temperature of 160°C. The curves corresponded to a broad distribution or bimodal peak at low reaction times; they became progressively narrower and shifted toward lower retention times, as shown in Figure 8, for the representative PLAH homopolymer. In this case, 90 min were required to obtain a polymer sample with the highest molecular weight. No improvement was observed when the reaction time was increased, but rather a worse distribution was observed when the time was close to 120 min because of the occurrence of some thermal degradation. It should be pointed out that chromatograms of samples obtained under optimized

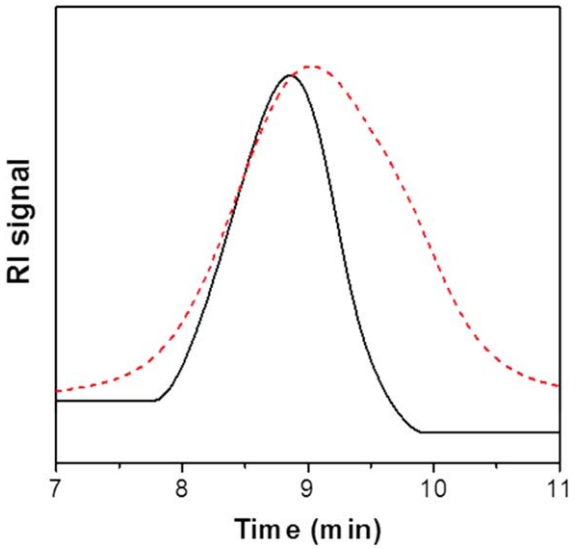

Figure 8. GPC chromatograms of the PLAH samples obtained after polymerization at 160°C for 15 min (dashed line) and 90 min (continuous line). Refractive index (RI) [Color figure can be viewed in the online issue, which is available at wileyonlinelibrary.com.]

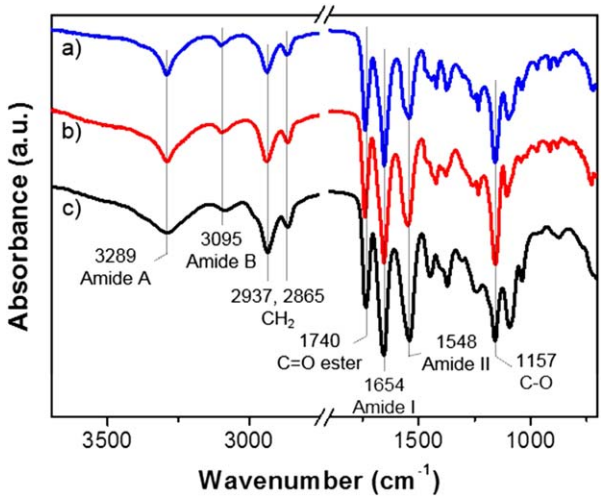

Figure 9. FTIR spectra of the representative samples: (a) PGAH, (b) P(GAH–LAH) 50, and (c) PLAH. [Color figure can be viewed in the online issue, which is available at wileyonlinelibrary.com.]

conditions did not show any peak indicative of low-molecular-weight fractions that would correspond to both unreacted and highly degraded samples.

Copolymerizations were also performed for 90 min because the added GAHK monomer reacted faster and, again, no degradation products were detected. Table IV shows that polymerization yield after purification was high (68–79%), with no specific trend being detected with the monomer composition. A great variation was found for the molecular weight because it decreased regularly from 26,000 to 11,500 g/mol as the LAHK ratio increased. This feature pointed out the limitation caused by the lower reactivity of LAHK and the unfeasibility of prolonging the reaction time. Experimental polydispersity indices were similar for all of the samples (1.9–2.4); the mean value was in agreement with that expected for a typical polycondensation reaction distribution.

Figure 9 shows the FTIR spectra of the PGAH and PLAH homopolymers and the representative copolymer obtained from an equal ratio of both monomers. Typical ester (C═O, ~1740 cm^{-1}; C—O, ~1157 cm^{-1}), amide (A, ~3289 cm^{-1}; B, ~3095 cm^{-1}; I, ~1654 cm^{-1}; II, ~1548 cm^{-1}) and methylene (2937 and 2865 cm^{-1}) bands were detected. The spectra were logically rather similar because the differences between the polymers only involved the change of the methylene group of the glycolic acid unit by the $CH(CH_3)$ group of the lactic acid unit. Nevertheless, the amide A and B bands were clearly broader in the PLAH sample; this suggested a greater difficulty with respect to the glycolic acid derivative in establishing hydrogen-bonding intermolecular interactions.

The ^{1}H-NMR and ^{13}C-NMR spectra were fully consistent with the expected chemical constitution, with all signals unambiguously assigned by means of two-dimensional HETCOR spectra (Figure 10). The ^{1}H-NMR spectra allowed us to determine the ratio of glycolic and lactic acid units incorporated into the synthesized samples; the resulting experimental values were in close agreement with the monomer feed ratio (Table IV). In particular, the molar content of glycolic units (also equivalent to GAH) and lactic acid (also equivalent to LAH) units were determined for each sample through consideration of the areas of

Table IV. Synthesis and Characterization Data for the Obtained Homopolymers and Copolymers

Sample	Yield (%)	GAH ratio (%)[a]	M_w (g/mol)	Polydispersity index	T_m (°C)[b]	ΔH_m (J/g)[b]	T_c (°C)[c]	T_g (°C)
PGAH	75	100	26,000	2.3	157, 148	77, 64	102, 124	16
P(GAH-LAH) 80	78	85	18,200	2.0	141, 143	75, 45	85, 86	19
P(GAH-LAH) 50	70	54	13,000	2.3	114, —	58, —	—	23
P(GAH-LAH) 20	68	22	12,000	2.4	85, —	9, —	—	25
PLAH	79	0	11,500	1.9	141, —	1, —	—	30

M_w: Molecular weight; T_m: Melting temperature; ΔH_m: Enthalpy of fusion; T_c: Crystallization temperature; T_g: Glass transition temperature.
[a] From the ^{1}H-NMR spectra.
[b] The left and right values correspond to the first and second heating runs, respectively.
[c] The left and right values are the crystallization temperatures from the cooling run and third heating run, respectively.

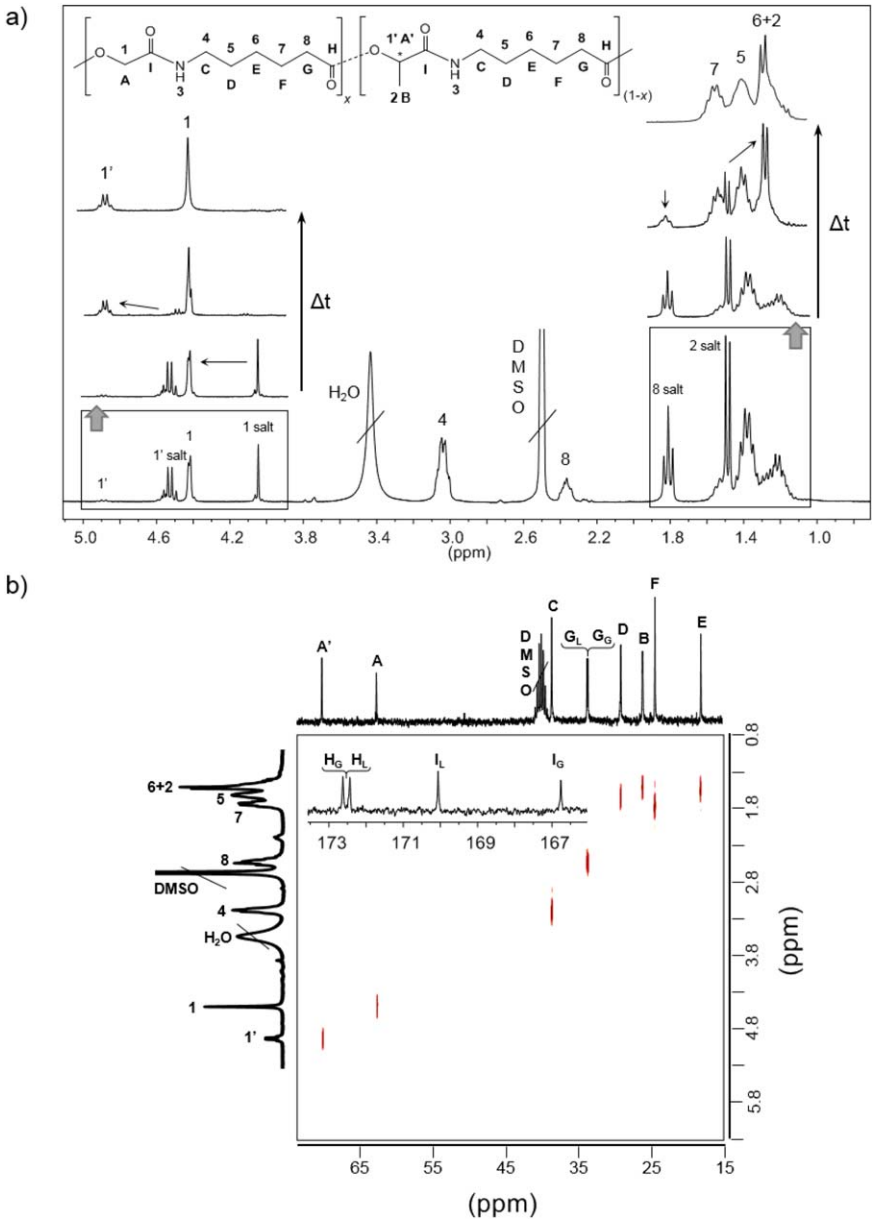

Figure 10. (a) ^{1}H-NMR spectra taken during the polymerization of the representative M(GAHK–LAHK) 50 monomer mixture at 160°C. (b) HETCOR two-dimensional spectra of the P(GAH–LAH) 50 purified sample. The inset shows the 174–165-ppm region of the ^{13}C-NMR spectra where the carbonylic signals of ester and amide groups appear. [Color figure can be viewed in the online issue, which is available at wileyonlinelibrary.com.]

the OCH_2CO ($A_{4.5–4.3}$) and $OCH(CH_3)CO$ ($A_{5.0–4.8}$) signals related to the methylene group of the glycolic acid unit and the methine group of the lactic unit, which appeared in the 5.0–4.3-ppm range, respectively:

$$\text{GAH ratio (\%)} = 100 \times A_{4.5–4.3}/[A_{4.5–4.3}+A_{5.0–4.8}] \quad (3)$$

The ^{1}H-NMR spectra were also useful for determining the optimum polymerization time for each monomer mixture; an example is shown in Figure 10(a) with the representative M(GAH–LAH) 50 mixture. It was clear that the intensity of signals corresponding to the CH_2COO^- and $CH(CH_3)COO^-$ protons (called the **1** and **1′** salts, respectively) progressively diminished with the reaction time until they finally disappeared, whereas the corresponding esterification peaks (**1** and **1′**) appeared and increased in intensity until the reaction was completed. The time required to achieve an invariable spectrum without distinctive monomer salt signals was in agreement with previous GPC and FTIR observations.

In addition, the section between 1.9 and 1.0 ppm was also worth monitoring because two peaks corresponding to the potassium salt monomers could be clearly distinguished. These corresponded to the $ClCH(CH_3)CO$ methyl proton (called the **2** salt) and the $CH_2COO^-K^+$ methylene proton (called the **8** salt) that were close to chlorine and carboxylate terminal groups. The time evolution of the spectra showed the decrease in these monomer signals and the progressive increase in related signals

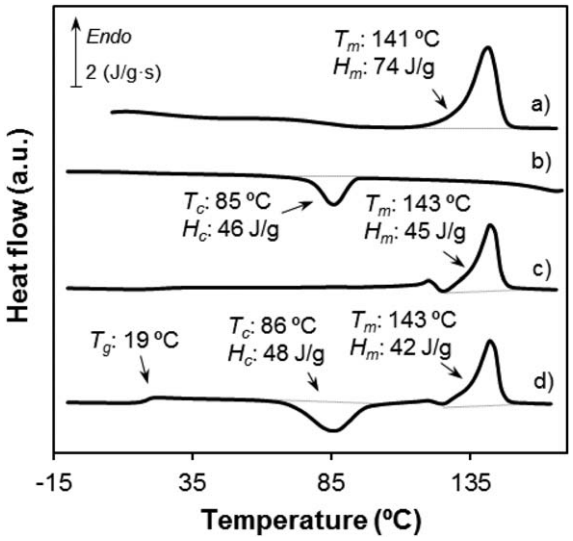

Figure 11. DSC traces obtained during the (a) heating run of the P(GAH–LAH) 80 sample, (b) cooling run from the melt state, (c) heating run of the previously crystallized sample, and (d) heating run of a sample quenched from the melt state.

associated with the formed polymer (called **2** and **8**). The change in the former peak involved both GAHK and LAHK monomers, whereas the second one was only associated with the LAHK monomer.

^{13}C-NMR signals observed in the HETCOR correlation spectra [Figure 10(b)] also deserve attention because they made it possible for us to distinguish between the aminohexanoic units that were linked to the glycolic or the lactic acid residues. Specifically, the CH_2CO methylene carbon of the P(GAH–LAH) 50 sample (labeled **G** in Figure 10) appeared as a symmetric doublet centered at 33.28 ppm; this indicated the presence of equal ratios of neighboring lactic (L subscript) and glycolic (G subscript) units along the polymeric chain. In the same way, a splitting of the signal corresponding to the aminohexanoic carbonylic carbon was observed; this depended on the neighboring glycolic or lactic acid unit [inset of Figure 10(c)]. Unfortunately, the spectra were not sensitive to triad sequences, and consequently, no information concerning the microstructure (e.g., random or blocky distribution) could be derived.

Thermal Properties of the P(GAH–LAH) Copolymers

The thermal properties of the new PLAH and copolymer samples were studied by DSC, as summarized in Table IV, according to the protocol shown for a representative semicrystalline copolymer in Figure 11. The most interesting features are highlighted as follows:

1. The glycolic and lactic acid residues were miscible in the amorphous phase independently of their ratio because a single glass-transition temperature was always observed. This temperature gradually increased from 16 to 30°C with the increase in lactic acid units, as expected from the incorporation of the methyl lateral groups, which hindered chain mobility.
2. Crystallization was hindered by the incorporation of the racemic lactic acid units. In this way, samples with an LAH acid content equal to or higher than 50% were not able to crystallize from the melt state. In the same way, the melting enthalpy of the synthesized samples decreased from 77 to 1 J/g with the LAH acid content. The same trend could be deduced from the decrease in the crystallization temperature (from both the melt and the glassy state), although in this case, data could not be obtained from the samples having an LAH acid content of higher than 20%.
3. The copolymers showed a clear melting point decrement with respect to the pure PGAH or PLAH homopolymers as a logical consequence of the increasing comonomer content. Thus, a minimum melting temperature of 85°C was found at an intermediate composition in contrast to the values of 157 and 141°C determined for the PGAH and PLAH homopolymers, respectively. This eutectic behavior was highly meaningful because it suggested isodimorphism, a feature that enables the incorporation at each crystalline phase of the corresponding comonomer. It is known that an eutectic melting point is frequently observed in random copolymer crystallization, and consequently, it may have proven that an effective copolymerization was achieved in the thermal polycondensation process.

Thermogravimetric traces of the purified polymers (Table V) were logically similar to those obtained from the corresponding monomer mixtures (Table II and Figure 3) when we took into account the fact that the removal of the inorganic KCl salt led to a lower residual weight. In any case, a significant organic char yield was found, and specifically, it steadily increased from 9.7 to 16.8% with the lactic acid content. It was also remarkable that the onset degradation temperature of the polymers varied in a narrow temperature range (248–265°C) that was higher enough than their melting temperature to allow their processing from the melt state.

Table V. Characteristic TGA Temperatures, Remaining Weights, and DTGA Peak Values for the Decomposition of the Different Homopolymers and Copolymers Obtained

Polymer	T_{onset} (°C)	$T_{10\%}$ (°C)	$T_{20\%}$ (°C)	$T_{40\%}$ (°C)	w_t (%)	T_1 (°C)	T_2 (°C)
PGAH	256	314	330	359	9.7	335	433
P(GAH-LAH) 80	261	319	334	365	9.7	339	436
P(GAH-LAH) 50	265	316	331	354	12.0	334	434
P(GAH-LAH) 20	260	314	335	364	14.5	342	430
PLAH	248	304	324	352	16.8	335	401

T_1 and T_2, the two temperatures observed in the DTGA traces.

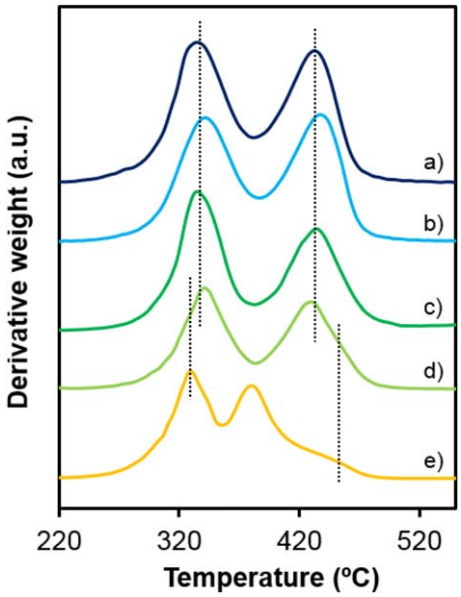

Figure 12. DTGA traces of (a) PGAH, (b) P(GAH–LAH) 80, (c) P(GAH–LAH) 50, (d) P(GAH–LAH) 20, and (e) PLAH. [Color figure can be viewed in the online issue, which is available at wileyonlinelibrary.com.]

Polymer degradation always took place according to the previously indicated two-step decomposition process, and therefore, two predominant peaks were clearly detected in the DTGA curves (Figure 12). The first one corresponded to a similar temperature for all of the samples, whereas the second one appeared at a significantly lower temperature for PLAH. Hence, the degradation products of lactic acid units favored the decomposition process of the aminohexanoic acid residue, as also observed from the decomposition curve of monomers. Nevertheless, slight differences were observed between the thermogravimetric curves of the purified polymers and the related monomers because in the last case, the decomposition processes were detected at higher temperatures; this suggested that inorganic salt particles may have hindered the leakage of degradation products.

CONCLUSIONS

New PEAs incorporating lactic acid units were prepared easily by the thermal polycondensation process of a metal salt of a chloro-2-propionate derivative (i.e., LAHK). Polymers were obtained with high yield but with moderate molecular weights since reaction time should be limited due to degradation processes. These took place at the high temperature required to favour the polycondensation reaction. The reactivity of the lactic acid derived monomer was lower than the related monomer having a glycolic acid unit. Kinetic analysis demonstrated that the differences in the polymerization rate of these monomers increased drastically with the reaction temperature but were still acceptable at 160°C for conducting an effective copolymerization process.

The new copoly(ester amide)s showed a good miscibility in the amorphous state between the lactic acid and glycolic acid units and properties that were dependent on the composition. Therefore, characteristics, such as the degree of crystallinity, melting point, and glass-transition temperature, could be tuned as the function of the monomer–salt ratio used in a polycondensation process that had as a driving force the formation of metal halide salts. The melting temperature of the copolymers showed a eutectic behavior that supported the achievement of an incompletely blocky microstructure, as also expected from the variation of the exothermic polymerization temperatures when monomer mixtures were used instead of single monomers. Copoly(ester amide)s and the related homopolymers could be processed from the melt state, as their decomposition temperatures were considerably higher than the corresponding melting temperatures.

ACKNOWLEDGMENTS

The authors are indebted to Ministerio de Economıa y Competitividad (MINECO) and Fondo Europeo de Desarrollo Regional (FEDER) (contract grant number MAT2012-36205) and the Generalitat de Catalunya (contract grant number 2009SGR1208) for their support. One of the authors (S.K.M.) acknowledges an Formación del Personal Investigador (FPI) grant from Ministerio de Ciencia e Innovación (MICINN).

REFERENCES

1. Epple, M.; Kirschnick, H. *Chem. Ber.* **1996**, *129*, 1123.
2. Schwarz, K.; Epple, M. *Macromol. Chem. Phys.* **1999**, *200*, 2221.
3. Herzberg, O.; Epple, M. *Eur. J. Inorg. Chem.* **2001**, 1395.
4. Epple, M.; Kirschnick, H. *Liebigs Ann.* **1997**, 81.
5. Takao, Y.; Kasashima, Y.; Inoki, M.; Akutsu, F.; Naruchi, K.; Yamaguchi, Y. *Polym. J.* **1995**, *27*, 766.
6. Siedler, M.; Kitchin, S. J.; Harris, K. D. M.; Lagoa, A. L. C.; Diogo, H. P.; Minas da Piedade, M. E.; Epple, M. *J. Chem. Soc. Dalton Trans.* **2001**, 3140.
7. Rodriguez-Galan, A.; Vera, M.; Jimenez, K.; Franco, L.; Puiggali, J. *Macromol. Chem. Phys.* **2003**, *204*, 2078.
8. Vera, M.; Rodríguez-Galán, A.; Puiggalí, J. *Macromol. Rapid Commun.* **2004**, *25*, 812.
9. Okada, M. *Prog. Polym. Sci.* **2002**, *27*, 87.
10. Lips, P. A. M.; Dijkstra, P. J. In Biodegradable Polymers for Industrial Applications; Smith, R., Ed.; Elsevier: Cambridge, England, **2005**; p 107.
11. Rodriguez-Galan, A.; Franco, L.; Puiggali, J. *Polym. (Basel)* **2011**, *3*, 65.
12. Murase, S. K.; Puiggalí, J. In Natural and Synthetic Biomedical Polymers; Kumbar, S. G., Laurencin, C. T., Deng, M., Eds.; Elsevier: Amsterdam, **2014**; p 145.
13. Vera, M.; Franco, L.; Puiggalí, J. *J. Polym. Sci. Part A: Polym. Chem.* **2008**, *46*, 661.
14. Murase, S. K.; Franco, L.; del Valle, L. J.; Puiggalí, J. *J. Appl. Polym. Sci.* **2014**, *131*, 40102.

15. Murase, S. K.; Franco, L.; Rodríguez-Galán, A.; Puiggalí, J. *J. Appl. Polym. Sci.* **2012**, *126*, 1425.
16. Botines, E.; Franco, L.; Puiggalí, J. *J. Appl. Polym. Sci.* **2006**, *102*, 5545.
17. Vera, M.; Admetlla, M.; Rodríguez-Galán, A.; Puiggalí, J. *Polym. Degrad. Stab.* **2005**, *89*, 21.
18. Zhiyong, Q.; Sai, L.; Hailian, Z.; Xiaobo, L. *Colloid Polym. Sci.* **2003**, *281*, 869.
19. Lu, D.; Ren, Z.; Zhou, T.; Wang, S.; Lei, Z. *J. Appl. Polym. Sci.* **2008**, *107*, 3638.
20. Vera, M.; Franco, L.; Puiggalí, J. *Macromol. Chem. Phys.* **2004**, *205*, 1782.